Chapter II.8
Observations of the Lower Atmosphere Over West Africa Using Ground-Based Remote Sensing Instruments

Bernhard Pospichal and Susanne Crewell

1 Introduction

Weather and climate over tropical West Africa are determined by the annual cycle of the West African monsoon, which is an annual reversal of the lower tropospheric flow pattern between the moist southwesterly monsoon flow and the dry northeasterly Harmattan flow (Hastenrath 1985). At the beginning of the monsoon season in March/April, the inter-tropical convergence zone (ITCZ) moves inland, reaching its northernmost point in July and August. The ITCZ marks the upward branch of the Hadley cell and the maximum of tropospheric water vapor convergence. It is situated at the equator (Gulf of Guinea) in January and moves north to about 11°N in August. The ITCZ is not to be confused with the inter-tropical discontinuity (ITD) which marks the convergence zone between the low level flows. The ITD is always situated north of the ITCZ (at about 7°N in December/January and 20°N in July/August). The ECMWF analysis of April 10, 2006 (Fig. II.8.1) presents the sharp meridional moisture contrasts along the ITD which was at about 10°N at that time. At the same time, the integrated water vapor (IWV) maximum at about 5°N marks the ITCZ. It was most pronounced over the Atlantic Ocean. Rainfall also shows an annual cycle with a very pronounced rainy season becoming shorter and less regular when moving north.

The mechanisms that influence the observed inter-annual variability of the West African Monsoon are still not well understood. The African Monsoon Multidisciplinary Analysis (AMMA) project has been launched to gain a deeper insight into this question by combining a wide variety of ground-based, maritime, airborne, and satellite measurements (Redelsperger et al., 2006). Atmospheric humidity plays a key role in those processes that determine the strength of the monsoon. A very significant part of the atmospheric water – whether liquid or as water

B. Pospichal (✉)
University of Cologne, Cologne, Germany
e-mail: pospichal@meteo.uni-koeln.de

D. Cimini et al. (eds.), *Integrated Ground-Based Observing Systems*,
DOI 10.1007/978-3-642-12968-1_15,

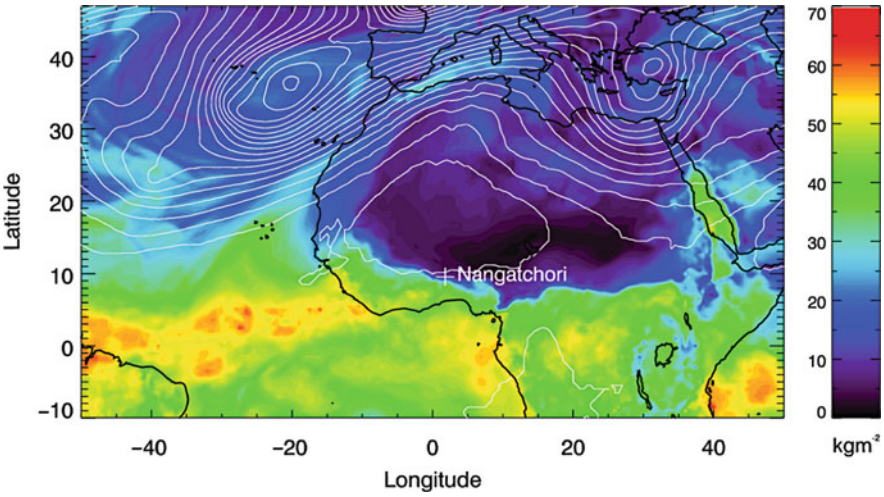

Fig. II.8.1 Synoptic situation on April 10, 2006, 00 UTC from ECMWF analysis. Integrated water vapor (*shaded*) and 500 hPa geopotential height (*contour lines* with 20 gpm distance) are shown

vapor – is located in the atmospheric boundary layer (ABL). For this reason, the observation of the lowest part of the atmosphere is essential to get a comprehensive view of the monsoon.

Observations are rather sparse in West Africa. In the past some campaigns, e.g., HAPEX-Sahel in 1992 (Dolman et al., 1997) and Jet 2000 (Thorncroft et al., 2003) have provided more detailed observations by aircraft, enhanced radiosoundings, pilot balloons, and in situ surface stations. Since all these data are confined to limited time intervals, Parker et al. (2005) note the complete lack of measurements with high temporal resolution in that region. This deficit can also not be closed through satellite observations as those measurements do not resolve the ABL adequately. Within AMMA a wealth of observations was gathered during special observation periods of a few months and longer term observations for a period of 1 year or more were installed. One example is the radiosounding network which has been extended as part of AMMA, but even then, most of the stations performed soundings only 2–4 times a day at the main synoptic hours with a spacing of about 500 km between the stations.

2 Instrumentation

In order to fill the gap of detailed observations in West Africa AMMA initiated – amongst others – the setup of the Djougou/Nangatchori site where a variety of remote sensing and in situ instruments were installed (Pospichal and Crewell, 2007). Nangatchori is situated in northwestern Benin (9.6°N, 1.8°E, 435 m MSL,

Fig. II.8.1). The rainy season typically starts there in late April and lasts until mid-October. The month with the highest amount of rain is August.

Continuous thermodynamic monitoring of the lower troposphere was performed in 2006 by a novel ground-based microwave radiometer the Humidity And Temperature PROfiler HATPRO (Rose et al. 2005) with high temporal resolution. Compared to other microwave radiometers HATPRO is able to observe temperature profiles with high vertical resolution in the atmospheric boundary layer through scanning (Löhnert and Crewell, 2003) in addition to the standard products, e.g., IWV, LWP (cloud liquid water path), and full troposphere temperature and humidity profiles. To our knowledge, this has been the first time that such a microwave radiometer was used in West Africa for monitoring the lower troposphere. Additional instruments at Nangatchori include a lidar ceilometer, vertical pointing Doppler rain radar, measurements of temperature, humidity, and wind on a tower at five levels up to 6 m height, a rain gauge network, detailed in situ and remote sensing aerosol observations (Pelon et al., 2008), wind profiler, and ozone lidar.

The instrument setup was very well suited to describe the lower atmosphere in much detail, both temporally and vertically. The operations were conducted over a full year's cycle (January 12, 2006–January 22, 2007), with a data availability of 82% (HATPRO) to 92% (ceilometer) during this period. The downtime of HATPRO is due to power breaks, a mirror failure, and water contamination of the radome. A brief description of the instruments and the measurement parameters is given in Table II.8.1. HATPRO and ceilometer were tilted to the north in order to avoid

Table II.8.1 Instruments in Nangatchori in 2006 used for this study

Instruments	Frequencies	Measured parameters	Resolution/accuracies
Microwave radiometer RPG-HATPRO	Seven channels at H_20 absorption line (22.24–31.4 GHz) Seven channels at O_2 absorption complex (51.26–58.0 GHz)	• Fourteen channels microwave brightness temperatures (zenith obs., every 15 min elevation scanning) Derived parameters: • IWV (total column atmospheric water vapor content) • LWP (atmospheric liquid water path) • Temperature (T)and humidity (q) profiles	Temporal resolution: 2 s for zenith obs.,15 min for elevation scans Accuracies: • IWV: < 1 kg m^{-2} • LWP: 20–30 gm^{-2} • T-Profiles: 0.5 K at 500 m, decreasing to 2 K at 5 km (Crewell and Löhnert, 2007) • q-Profiles: not more than two independent layers can be detected
Lidar ceilometer Vaisala CT25 K	$\lambda = 905$ nm	• Vertical backscatter profiles up to 7.5 km AGL • Cloud base height (up to three layers can be detected)	Temporal resolution: 15 s Vertical resolution: 30 m

Table II.8.1 (continued)

Instruments	Frequencies	Measured parameters	Resolution/accuracies
Micro Rain Radar Metek	24.1 GHz	Vertical Doppler spectra (up to 4.8 km AGL) Derived parameters: • Drop size distribution • Fall velocity • Rain rate	Temporal resolution: 10 s Vertical resolution: 160–200 m (depending on measurement mode)
GPS receiver in Djougou (10 km west of Nangatchori)		Zenith tropospheric wet delay Derived parameter: • Integrated water vapor	Temporal resolution: 15 min. Accuracy 0.5 kg m^{-2} (Bock et al., 2008)

pointing directly into the sun during the course of the year. Although these measurements were performed under an elevation angle of 70°, we will later refer to them as "zenith."

In order to derive meteorological quantities from HATPRO brightness temperature measurements, statistical retrievals for IWV, LWP, temperature, and humidity profiles have been developed from radiosonde data. Due to a lack of sufficient high-quality soundings in West Africa, it was necessary to use radiosonde data from a region with similar climatic conditions. We chose to take northern Australia (Darwin, Gove) where nearly 15,000 sondes between 1990 and 2005 were available. Comparisons of Darwin climatology with soundings from Parakou in 2006 (100 km east of Nangatchori) confirm that the atmospheric states are quite similar.

3 Overview over Atmospheric Parameters in 2006 in Central Benin

3.1 Integrated Water Vapor (IWV)

The IWV during 2006 as derived by HATPRO and complemented by GPS measurements from Djougou (10 km east of Nangatchori; Bock et al., 2008) shows the strong variations between 10 and 50 kg m^{-2} (Fig. II.8.2). The dry season in early 2006 was characterized by several outbreaks of humid air from the south which resulted in large inter-diurnal variations of the atmospheric water vapor content and on average much moister conditions than normal. The diurnal mean of IWV varied between 15 and 43 kg m^{-2} before 15 April. During this period, two major rainfall events were observed (15 February and 23 March). In late April, the southerly monsoon flow became dominant in the area, resulting in IWV daily mean values of 40−50 kg m^{-2}, combined with more frequent rainfall events during this period. In

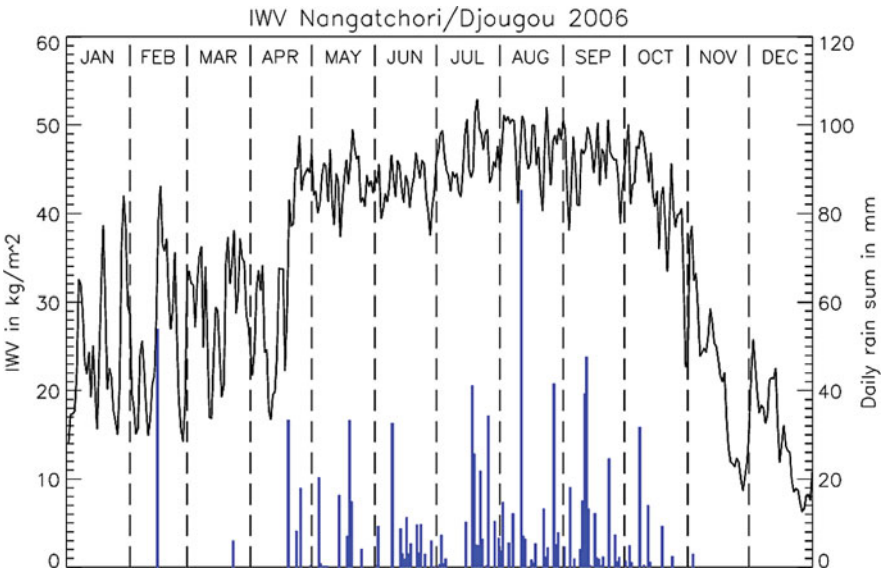

Fig. II.8.2 *Solid line*: Mean daily values of integrated water vapor (aggregate from HATPRO and GPS measurements). *Bars*: Daily rain amount in millimeter from Nangatchori

June 2006, there were only unusually few rain events. Finally, by mid-July heavy monsoon precipitation sets in. This occurred in conjunction with a slight increase in IWV values. By the end of September, precipitation started to diminish, associated with a decrease in IWV. After the last rain of the season on 2 November, the water vapor content continued to fall considerably from nearly 40 to less than 10 kg m^{-2} by the end of November. December was quite dry with IWV values between 7 and 25 kg m^{-2}, much in contrast to the dry season in January 2006. Measurements in January 2007 revealed much drier and cooler conditions also during that month compared to 2006 (not shown).

The high water vapor variability during the dry season is also presented in Fig. II.8.3. During the wet season (May–October 2006) 90% of the IWV observations range between 35 and 50 kg m^{-2}, whereas in the dry season (January–April and November–December 2006), the variation is much larger (90% of the observed values lie between 8 and 41 kg m^{-2}).

3.2 Clouds

To further investigate water cycle variables, the daily amount of cloud cover is plotted in Fig. II.8.4. The annual cycle of cloud cover follows the IWV cycle quite well with a maximum between July and September (Fig. II.8.2). However, even during dry season between January and March 2006, several days with 20–50% cloud cover can be identified. These days are connected with higher IWV values and also with a

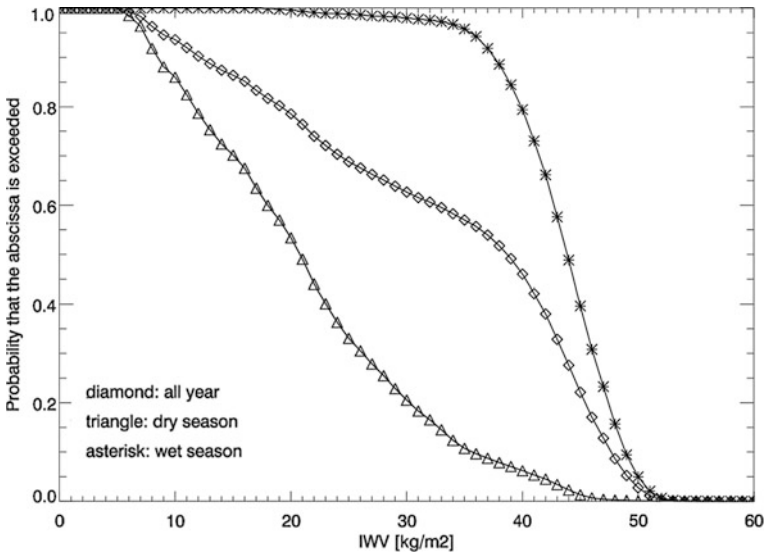

Fig. II.8.3 Cumulative frequency distribution of IWV from HATPRO measurements. Dry season: January–April and November–December 2006. Wet season: May–October 2006

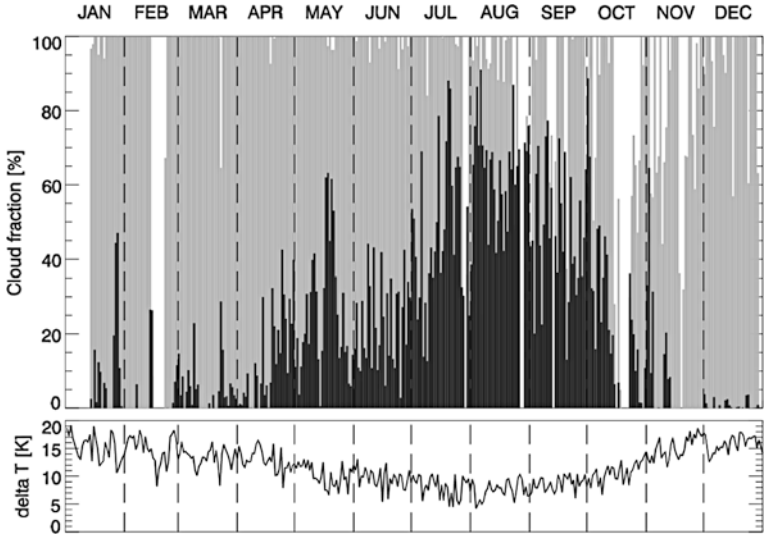

Fig. II.8.4 Fraction of the day (in percent) with cloud cover <7,500 m AGL (*black*), clear sky (*grey*), no data (*white*). *Lower part* shows the diurnal temperature range (T_{max}–T_{min})

lower diurnal temperature range (Fig. II.8.4, bottom). These periods are characterized by moist air from the south over the area. With the beginning of the wet season in late April, cloud cover rises significantly. A further increase of cloudy periods toward the end of July marks the beginning of the peak monsoon time. This is in good agreement with the higher rainfall amounts during that period (Fig. II.8.2). Until mid-October cloud cover remains fairly high, followed by a rapid decrease of clouds and moisture toward November. After 15 November, virtually no clouds have been detected. At that time, also the driest air masses for the whole year 2006 were observed over Nangatchori (Fig. II.8.2).

In order to demonstrate the impacts of clouds, Fig. II.8.5 presents the dependency of the diurnal temperature range with respect to the fraction of the day with clouds. Nearly all cloud-free days have a temperature range higher than 12 K, whereas on cloudy days with more than 50% clouds the difference between maximum and minimum temperature is mostly between only 5 and 10 K. These days are characteristic for the wet season when maximum temperatures are lower than during the dry season.

Cloud observations by ceilometer can also shed light on ABL development because ABL depth is often connected with the base of developing cumulus clouds. The mean diurnal cycle of cloud base height (Fig. II.8.6) is characterized throughout the whole year by a vertically developing ABL after the sun rises at around 6 UTC (Sunrise varies only between 5:31 and 6:15 UTC throughout the year). However, there are some significant differences between the seasons concerning the ABL depth. Before the onset of the monsoon (March/April) when cloud cover is sparse and the soil is dry, the large sensible heat flux over the whole day leads to strong ABL development with highest cloud bases (about 2,500 m) in the afternoon. The ABL becomes less deep in May/June (1,500 m) and reaches only up to about 1,000 m during July–October (peak of wet season). In addition, the amount of low night-time clouds (fog) is much larger at that time. In the end of the year hardly any

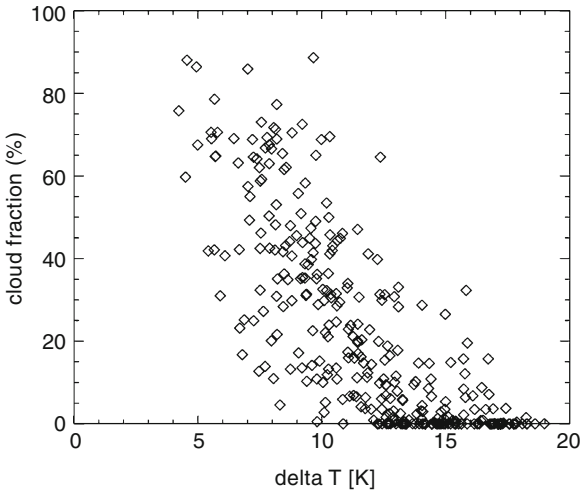

Fig. II.8.5 Scatterplot of diurnal 2-m temperature range (T_{max} minus T_{min}) and cloud cover for all days of 2006

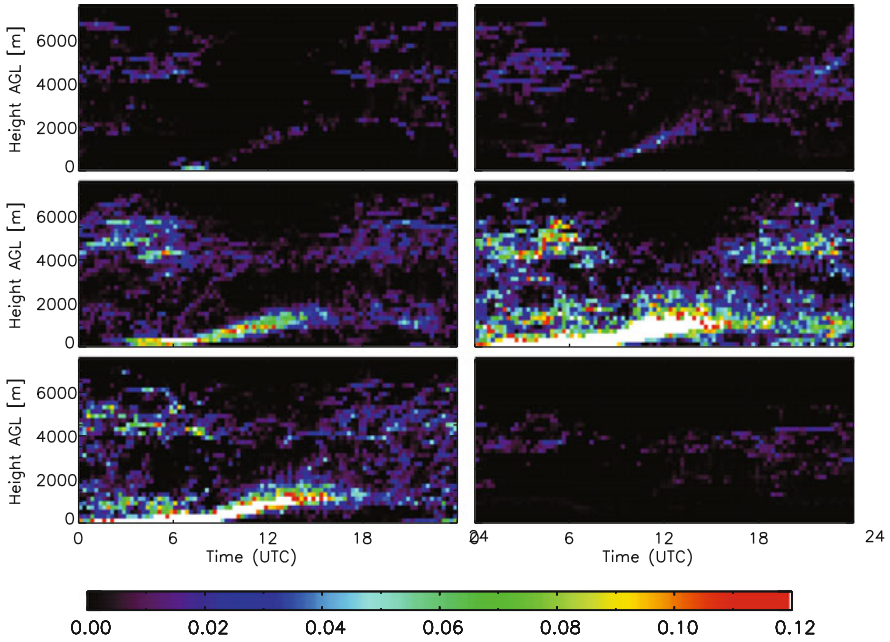

Fig. II.8.6 Diurnal cycle of cloud base heights in 2006 for six periods of 2 months each. Shading indicates the relative frequency of cloud base occurrence

clouds occur which is in no comparison with the dry season at the beginning of the year.

Another evident feature is a second cloud maximum in 4–6 km above ground which can be detected throughout all seasons. These clouds are presumably connected with the African Easterly Jet which has its maximum in about 4 km above ground and are mainly present during night as shown in Fig. II.8.6. However, this might be artificial since the distribution of medium to high clouds is somewhat influenced by the presence of opaque low clouds which cannot be penetrated by the ceilometer, making the detection of higher clouds impossible.

3.3 Cloud Liquid Water Path (LWP)

Microwave radiometry is by far the most accurate method to remotely sense the amount of cloud liquid water and therefore provides a unique opportunity to view the statistical distribution of cloud liquid water for all 2006 (Fig. II.8.7). LWP values above 1,000 gm^{-2} are very rare, but nevertheless, during rainy season some clouds with an LWP of up to 2,000 gm^{-2} were present over Nangatchori. Here it is important to note that only non-precipitating clouds are considered and that some high LWP events occurring after a rain event might be excluded due to a wet radome. In Table II.8.2, the percentage of HATPRO measurements with LWP values greater

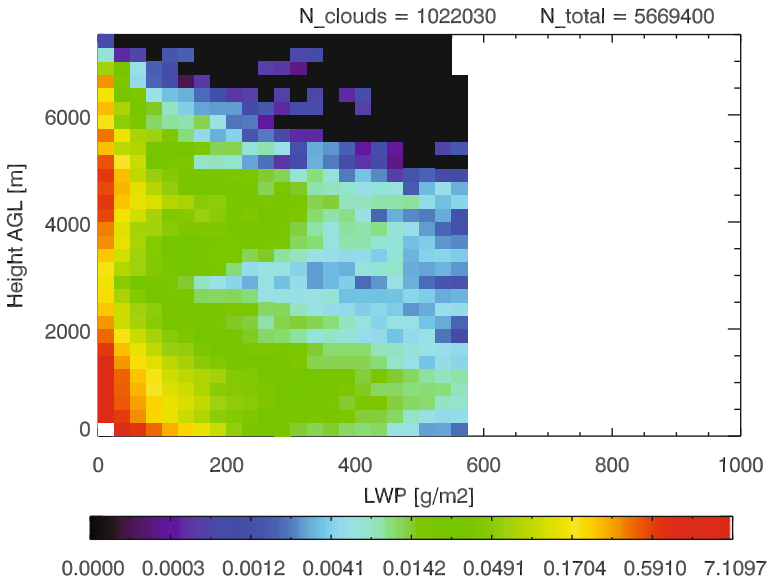

Fig. II.8.7 Frequency distribution of LWP (HATPRO) vs. cloud-base heights (ceilometer). The number of cloudy observations ($N_{\_clouds}$) as well as the total number of observations where both HATPRO and ceilometer operated (N_{total}) are shown at the top. Shading indicates the percentage of detected clouds relative to N_{clouds} for each particular bin (the maximum value being in lowest left bin)

than 10 gm^{-2} is indicated. This distribution is – as one should expect – well correlated with the cloud observations from the ceilometer (Fig. II.8.2). The highest monthly mean LWP was observed in August (75 gm^{-2}). The higher values of cloudy times between July and September are mainly due to HATPRO data gaps when the radome was wet.

The vertical distribution of LWP cannot be derived by microwave radiometry only. With the co-located ceilometer observations, it is possible to allocate a cloud-base height to each LWP measurement. Figure II.8.7 gives an overview of the distribution of cloud-base heights with respect to the corresponding LWP measurement. For this plot, all measurements in 2006 were used where LWP was greater than 0 gm^{-2} and clouds were detected by the ceilometer at the same time. Again two distinct cloud types are visible: boundary layer clouds and mid-tropospheric ones.

Table II.8.2 First line: Percentage of HATPRO measurements in 2006 with LWP > 10 gm^{-2}. Second line: Percentage of cloudy times, detected by the ceilometer

	Jan	Feb	Mar	Apr	May	Jun	Jul	Aug	Sep	Oct	Nov	Dec
LWP (%)	11	–	9	10	21	18	34	44	30	18	8	8
Clouds (%)	10	4	5	13	26	23	47	64	48	26	7	1

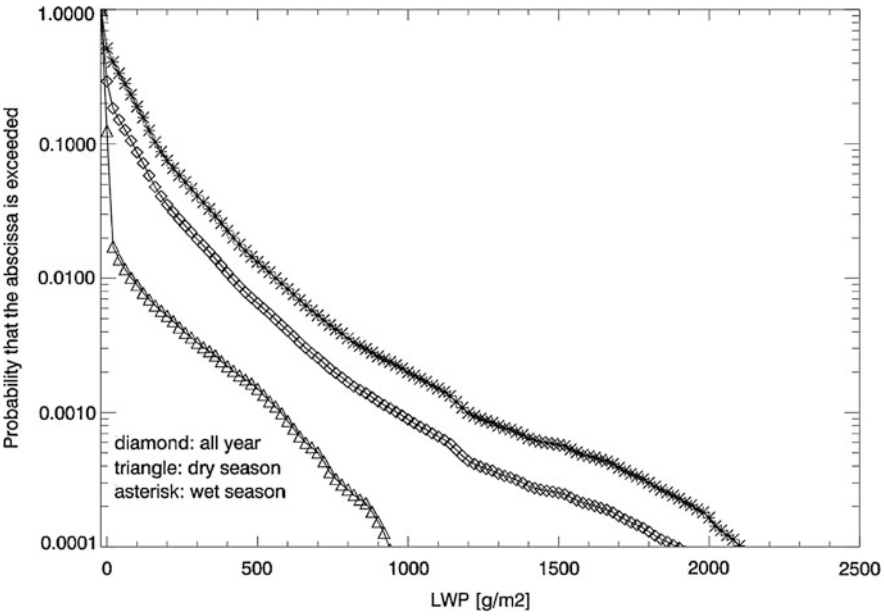

Fig. II.8.8 Frequency distribution of LWP from HATPRO measurements. Dry season: January–April and November–December 2006. Wet season: May–October 2006

Similar to water vapor a strong difference between dry and wet seasons is visible in LWP (Fig. II.8.8). During the dry months only 1% of the HATPRO measurements exceeded LWP values of 100 gm^{-2}, whereas in the wet season 20% of the time LWP was higher than 100 gm^{-2}. During wet season 1% of the values lay even beyond 550 gm^{-2}.

3.4 Temperature Profiles

From HATPRO measurements throughout the year, tropospheric temperature profiles with high temporal resolution could be derived, using a statistical retrieval algorithm which includes also elevation scans for the opaque frequencies close to the oxygen line. Generally, temperatures in the tropics do not change much in the course of the year, but there were some interesting features which could be observed here. The main differences between dry and wet season are captured by the profiles of potential temperature (theta) (Fig. II.8.9). During dry season (January–April and November–December), well-mixed conditions with adiabatic lapse rate (constant theta) prevailed in the afternoon, and a strong nocturnal temperature inversion (highly stable atmosphere) due to efficient radiative cooling is present. The depth of the well-mixed ABL (January–April > 2,000 m, July–September only about 700 m) is consistent with Fig. II.8.6.

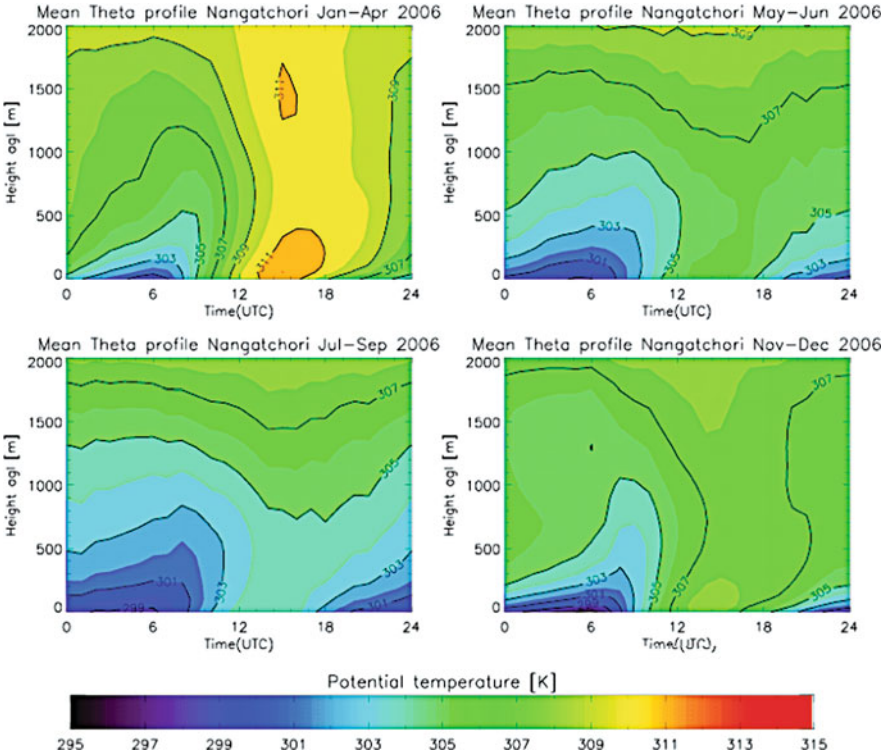

Fig. II.8.9 Mean potential temperature profiles for four different periods in 2006

In order to illustrate the diurnal cycle in more detail the mean diurnal cycle of potential temperature in 50 m above ground is shown for every month (Fig. II.8.10a). The largest diurnal temperature differences are present in dry season months when surface heating is strongest. This diurnal cycle is strongly reduced at 700 m above ground (Fig. II.8.10b) due to mixing processes. The differences between the warmest and the coldest months in 2006 are about 5 K. Fig. II.8.11 gives an overview over the inversion strength in the lowest 700 m of the atmosphere. During wet season the mean monthly theta difference does not exceed 5 K, being relatively constant throughout the night. In contrast, the dry season inversion strength increases until sunrise (6 UTC), the largest values being in November up to 9 K in monthly mean. This is due to the lower water vapor load which leads to less downwelling thermal radiation. In the afternoon, these values are reversed. During wet season the atmosphere is well mixed with basically no gradient in potential temperature between 0 and 700 m above ground. In dry season, for the lowest layers, superadiabatic conditions were observed due to the strong surface heating during daytime.

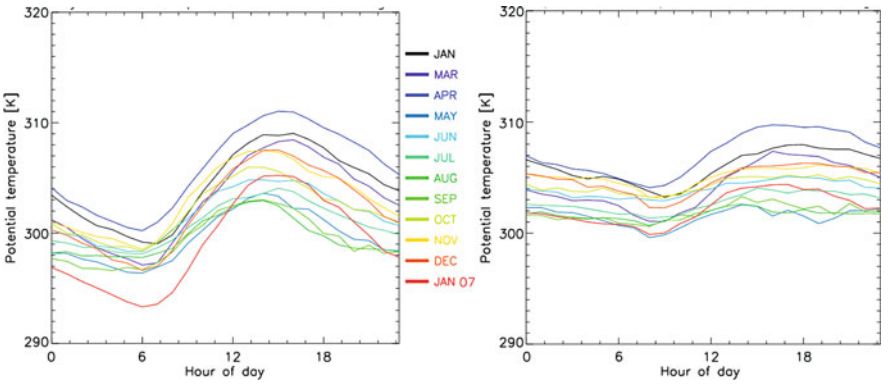

Fig. II.8.10 **a** (*left*): Diurnal cycle of potential temperature in 50 m above ground **b** (*right*): Same for 700 m above ground

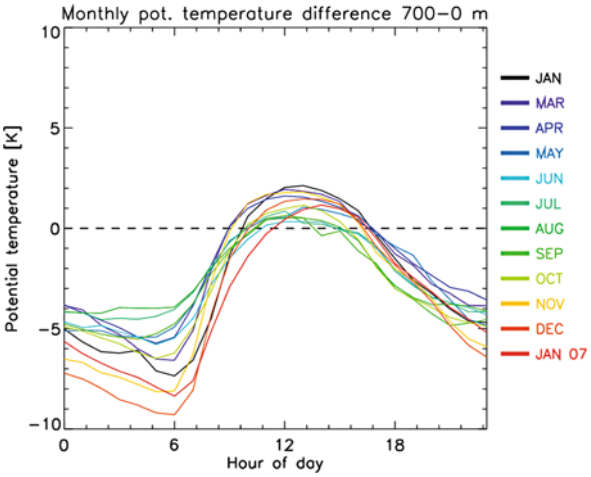

Fig. II.8.11 Diurnal cycle of potential temperature difference between 700 m above ground and the surface for different months of 2006

4 Diurnal Cycle of the Inter-Tropical Discontinuity (ITD)

The diurnal cycle of atmospheric processes around the ITD is recognized to be a key factor for the meridional transport of humidity in West Africa. A detailed overview of previous research is given by Parker et al. (2005) which is briefly summarized in the following: During daytime a heat low develops over the Sahara with a pressure minimum in the afternoon. As the convective boundary layer grows during the day, vertical mixing prevails and the horizontal flow is rather weak. In the late afternoon when sensible heating diminishes, turbulence stops rapidly and the flow is able to respond to the heat-low pressure gradient force. The low-level southerly flow intensifies over night and its edge moves northward. This nocturnal meridional flow is responsible for the advection of moist air in low levels further inland and

forms the main moisture source for summertime convection in the Sahel. In higher regions around 700 hPa there is a dry return flow. By day the low-level humidity falls, as dry air from above is mixed down in the developing convective boundary layer. When the ITD moved northward over Nangatchori, a distinct diurnal cycle of the ITD could be observed during 16 nights between April 1 and April 18, 2006 (Pospichal and Crewell, 2007). The meridional extent of this diurnal cycle is 100–200 km. During the night, the front between the moist monsoon air and the dry Harmattan air moves northward.

The continuous measurements of the HATPRO microwave profiler turned out to be a very good means to describe these processes with a high temporal as well as vertical resolution. In Fig. II.8.12, profiles of temperature, relative humidity, potential temperature, and equivalent potential temperature for the night of April 9/10, 2006 are presented. During the afternoon (12–18 UTC), a well-mixed layer with relatively low humidity values is present. After sunset at 1803 UTC, when the vertical turbulent mixing has stopped, dry air is advected from the northeast by the Harmattan flow, resulting in a decrease of relative humidity and equivalent potential temperature. On the contrary the temperature remains constant, except for a shallow layer close to the ground where an inversion has formed. Shortly after 00 UTC, the moist monsoon air arrives at Nangatchori. The temperature in the lowest 500 m diminishes by about 5 K, whereas humidity increases nearly instantaneously. Until sunrise (at 0545 UTC), the moist layer becomes deeper. After sunrise, vertical mixing starts

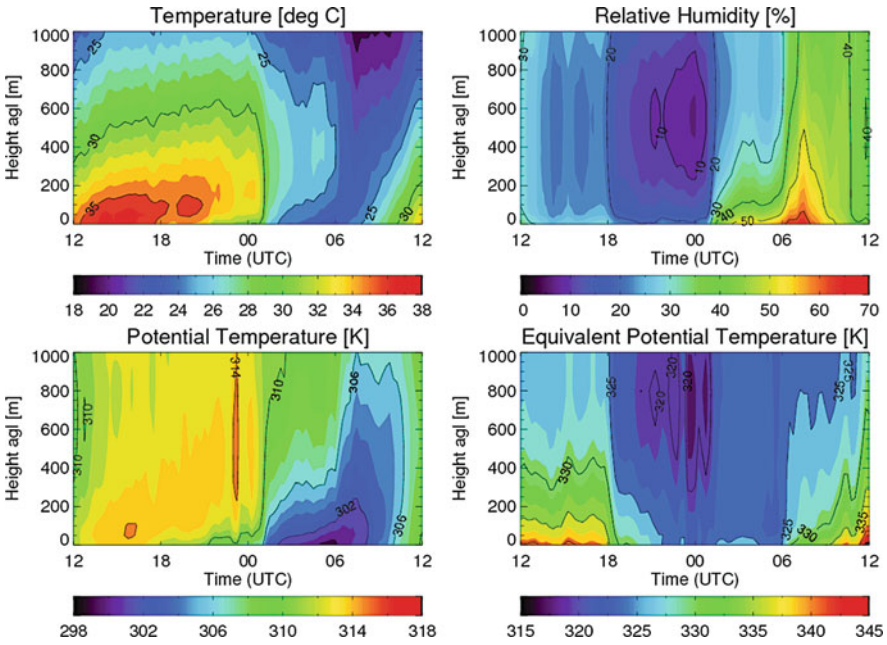

Fig. II.8.12 24-h cross sections of temperature, relative humidity, potential temperature, and equivalent potential temperature over Nangatchori on April 9/10, 2006. All measurements are derived from HATPRO measurements

and the moist and cool air is distributed vertically and at 12 UTC, the conditions are again nearly the same as 24 h before.

5 Conclusions and Outlook

During the whole year 2006, several ground-based remote sensing instruments were operated at Nangatchori (Benin) to study the conditions in the lower atmospheric levels with respect to the West African monsoon cycle. For the first time, continuous measurements with a microwave profiler and a ceilometer have been performed in this region. The instrument setup turned out to be a very good means to describe the atmospheric boundary layer with high temporal resolution. The deployment for one whole year made it possible to describe the complete annual cycle of cloud cover, IWV, LWP, and temperature profiles. Furthermore, a distinct diurnal cycle, connected with the northward move of the ITD before the onset of the wet season, was observed and could be used to evaluate a mesoscale model (Pospichal et al., 2010).

In the framework of AMMA, a similar data set of ground-based remote sensing observations has been collected at Niamey (Niger, 13.5°N, 2.1°E) which is located 400 km north of Nangatchori. At that location the mobile facility of the Atmospheric Radiation Measurement (ARM) Program was deployed (Miller and Slingo, 2007). A similar examination of these data is planned to get information on the meridional differences over West Africa, as Niamey represents a drier region with a much shorter rainy season and more dominant Harmattan winds throughout the year.

The 2006 measurements in Nangatchori continued until January 22, 2007. The first month of 2007 showed special conditions which were rather different to 2006. Dry air masses and a strong Harmattan flux were dominant in this month, resulting in unusually dry conditions even further south (3 weeks of dry air in Cotonou at the Guinean coast from December 31, 2006–January 22, 2007). In Nangatchori, this month was considerably cooler and drier than January 2006. This indicates that only continuous observations over a longer time period can provide information over inter-annual fluctuations. Evaluation of long-term monitoring would be necessary to understand more deeply the mechanisms that are responsible for inter-annual variability of the West African Monsoon.

Acknowledgments Based on a French initiative, AMMA was built by an international scientific group and is currently funded by a large number of agencies, especially from France, the UK, the USA, and Africa. It has been the beneficiary of a major financial contribution from the European Community's Sixth Framework Research Programme. Detailed information on scientific coordination and funding is available on the AMMA International Web site http://www.amma-international.org.

References

Bock O, Bouin MN, Doerflinger E, Collard P, Masson F, Meynadier R, Nahmani S, Koité M, Gaptia Lawan Balawan K, Didé F, Ouedraogo D, Pokperlaar S, Ngamini JB, Lafore JP, Janicot S, Guichard F, Nuret M (2008) The West African monsoon observed with ground-based GPS receivers during AMMA. J Geophys Res. doi:2008JD010327

Crewell S, Löhnert U (2007) Accuracy of boundary layer temperature profiles retrieved with multi-frequency, multi-angle microwave radiometry. IEEE Trans Geosci Remote Sens 45(7): 2195–2201. doi:10.1109/TGRS.2006.888434

Dolman AJ, Culf AD, Bessemoulin P (1997) Observations of boundary layer development during the HAPEX-Sahel intensive observation period. J Hydrol 189:998–1016

Hastenrath S (1985) Climate and circulation of the tropics. D. Reidel Publishing Company. Dordrecht, Boston. 455 pp

Löhnert U, Crewell S (2003) Accuracy of cloud liquid water path from ground-based microwave radiometry. Part I: dependency on cloud model statistics and precipitation. Radio Sci 38:8041. doi:10.1029/2002RS002654

Miller MA, Slingo A (2007) The arm mobile facility and its first international deployment: measuring radiative flux divergence in West Africa. Bull Am Meteorol Soc 88:1229–1244

Parker DJ, Burton RR, Diongue-Niang A, Ellis RJ, Felton M, Taylor CM, Thorncroft CD, Bessemoulin P, Tompkins AM (2005) The diurnal cycle of the West African monsoon circulation. Q J R Meteorol Soc 131:2839–2860

Pelon J, Mallet M, Mariscal A, Goloub P, Tanré D, Bou Karam D, Flamant C, Haywood J, Pospichal B, Victori S (2008) icrolidar observations of biomass burning aerosol over Djougou (Benin) during African monsoon multidisciplinary analysis special observation period 0: dust and biomass-burning experiment. J Geophys Res 113(D00C18). doi:10.1029/2008JD009976

Pospichal B, Crewell S (2007) Boundary layer observations in West Africa using a novel microwave radiometer. Meteorol Z 16:513–523

Pospichal B, Bou Karam D, Crewell S, Flamant C, Hünerbein A, Bock O, Said F (2010) Diurnal cycle of the inter-tropical discontinuity over West Africa analysed by remote sensing and mesoscale modelling. Q J R Meteorol Soc 136(S1):92–106. doi: 10.1002/qj.435

Redelsperger JL, Thorncroft CD, Diedhiou A, Lebel T, Parker DJ, Polcher J (2006) African monsoon multidisciplinary analysis: an international research project and field campaign. Bull Am Meteorol Soc 87:1739–1746

Rose T, Crewell S, Löhnert U, Simmer C (2005) A network suitable microwave radiometer for operational monitoring of the cloudy atmosphere. Atmos Res 75:183–200

Thorncroft CD, Parker DJ, Burton RR, Diop M, Ayers JH, Barjat H, Devereau S, Diongue A, Dumelow R, Kindred DR, Price NM, Saloum M, Taylor CM, Tompkins AM (2003) The JET2000 project: aircraft observations of the African easterly jet and African easterly waves. Bull Am Meteorol Soc 84:337–351